Delivery of Immunoreactive Antigen Using A Controllable Needle-Free Jet Injector

N. Catherine Hogan[a,*], Melis N. Anahtar[b], Andrew J. Taberner[c], and Ian W. Hunter[a]

[a]*BioInstrumentation Laboratory, Department of Mechanical Engineering, Massachusetts Institute of Technology, Cambridge, MA 02139, U.S.A.*
[b]*Harvard Medical School, Boston, MA 02115, U.S.A.*
[c]*Auckland Bioengineering Institute and Department of Engineering Science, University of Auckland, New Zealand*

*Corresponding author
Email: hog@mit.edu

Abstract

To assess the feasibility of immunizing mice against hepatitis B surface antigen (HBsAg), alum-adsorbed HBsAg was administered intradermally by jet injection or intradermally and subcutaneously using a 27G needle and syringe to mice. Three doses of antigen were delivered at 0, 14, and 28 days. Antibodies to HBsAg were detected only in mice injected with alum-absorbed HBsAg with antibody levels increasing with secondary injections. Mice vaccinated by intradermal injection using the jet injector or subcutaneous needle injection exhibited comparable immune responses at day 47. Differences in titer observed between intradermal jet injected and needle injected animals reflect differences in the volume of antigen delivered. With the exception of minor bleeding at the injection site in a few animals injected either by jet injection or needle, no adverse events were observed in any of the mice used in the study.

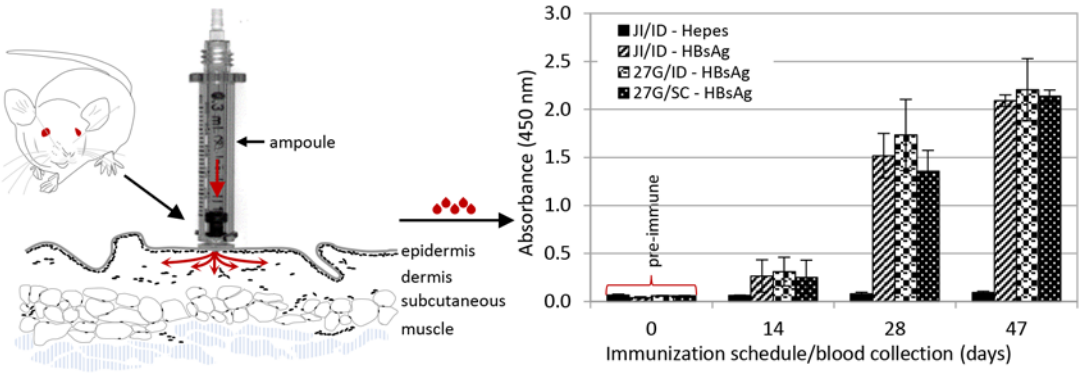

Graphical abstract: Intradermal injection of antigen using a controllable jet injector elicits an immune response comparable to that induced by needle and syringe.

Keywords
Needle-free, intradermal, HBsAg, immunization, jet injector, control

Introduction

Disease prevention is key to public health. Vaccines are routinely administered to induce immunologically-mediated resistance to a disease with many being administered intramuscularly (IM). However, given the role of Langerhans cells (LCs) and dendritic cells (DCs) in the initiation and regulation of the immune response to infectious pathogens [1], immunization strategies that target these cells may lead to more effective therapies [2][3][4][5].

There are several physical methods by which vaccines can be delivered to the skin, the most common method being the Mantoux technique [5][6][7]. Difficulties associated with reliable delivery using this method spurred the development of alternative technologies. Needle-free technologies capable of intradermal delivery include jet injection devices, microneedle arrays, and hollow needles to deliver solid or liquid vaccine formulations (For reviews, see [6][8][9][10]). Delivery of solid vaccines often requires formulation and processing technologies to create tiny rods or spray-dried powders, to coat particles or microneedles with solid drug, or to encapsulate the vaccine in biodegradable microneedles [9]. Stabilization techniques for individual vaccines often require customization with variable results [11].

Liquid jet injectors, on the other hand, typically require no re-formulation of the vaccine and have demonstrated efficacy in the delivery of a variety of inactivated, live-attenuated, recombinant subunit, and DNA vaccines [6][8]. Immune responses reported following vaccination using jet injectors are comparable (examples include [12][13][14] or, in some cases, enhanced [15][16][17] when compared to those elicited by conventional needles and syringes. Intradermal delivery of vaccines using jet injectors can result in dose sparing with some vaccines [18][19] and jet injection has been shown to be extremely effective in prime boost immunization regimens [20][21].

While intradermal delivery of vaccines has been demonstrated using spring-actuated devices, either designed specifically for the task [22][23][24] or coupled with an intradermal (ID) spacer [22][25], these devices afford no control over the pressure applied to the drug during delivery; the pressure-time profile is fixed. As such, species specific and gender-related differences in skin thickness and mechanical properties may limit their usefulness. More recent devices have used actuation mechanisms (*e.g.* piezoelectric actuators, voice coil actuators) that permit active control over the pressure applied to the drug during the injection thereby permitting improved control over both penetration depth and injection volume [26][27].

The linear Lorentz-force (voice coil) actuated jet injection system used in this study permits real time feedback control during the injection; the speed of the jet can be monitored and modulated continuously and the volume of fluid delivered regulated precisely. Varying the current input to the coil varies the force and pressure exerted on the drug, and permits us to tailor the velocity *vs.* time profile used for the injection. Such injection "trajectories" generally comprise two phases; the first phase defines both the initial jet velocity (v_{jet}) and the time (t_{jet}) for which this velocity need be sustained in order to puncture the tissue to a desired depth, while the second phase of delivery is characterized by a lower velocity (v_{follow} or v_{ft}), which is sustained for the time (t_{follow}) required to deliver the remaining drug volume [27].

This study discusses intradermal delivery of recombinant Hepatitis B surface antigen (HBsAg) to mice using a linear Lorentz-force (voice coil) actuated jet injector (JI) and compares the resultant immune response with that observed when the antigen is delivered

using a 27G needle and syringe (27G NS). Hepatitis B vaccine (HBV), the first vaccine produced by gene technology, provides protection against HBV, which is estimated by the WHO to result in 1 million deaths each year from HBV-associated liver cirrhosis or hepatocellular carcinoma (HCC)[28][29]. A device that provides an easier, potentially more reliable means of intradermal delivery of HBV could benefit persons exhibiting an impaired or absent response to intramuscular vaccination (*e.g.* due to Celiac or chronic kidney disease)[30][31] and more broadly vaccination programs where dose-sparing could prove critical to coverage (e.g. influenza, yellow fever, inactivated polio, or rabies vaccines)[3].

Materials and Methods

All experimental procedures were approved by the IUCAC at MIT and were conducted in accordance with the NIH Guide for the Use and Care of Laboratory Animals.

Injection device

Jet injections were performed using a commercially available ampoule (Injex30, Injex Equidyne) with a 300 µL capacity and mean nozzle diameter of 165 µm. The ampoule was attached to the front plate of a custom designed JI as described in [27]. The high-power actuator together with a real-time controller, power supply, and user interface permitted us to generate variable velocity injection trajectories and realize delivery of specific drug volumes at defined velocities to the specified target. Control over the volume and speed of drug delivered is accomplished via a position sensor and a closed loop position control algorithm informed by a feed-forward model of the system [27].

Determining injection parameters

Trajectories (i.e. velocity-time relations) providing the desired penetration and dispersion profiles in *ex vivo* tissue were required prior to *in vivo* delivery. Hemond *et al.* [32] had demonstrated that delivery of fluid to the skin and underlying tissue can be realized using a two phase injection trajectory and [27] showed that varying v_{jet} and t_{jet} influenced the depth of penetration of the jet while v_{follow} affected primarily the dispersion of fluid in the tissue. More recently, v_{follow} has been shown to influence penetration depth in addition to dispersion [33].

To date, the jet-injections reported using this approach have been for volumes ranging between 50 µL and 300 µL. Delivery to the upper dermal layer in mice required that a small volume of antigen (20 µL) be delivered to a depth of <1.0 mm. Because such a low-volume injection was completed in ≤25 ms, the need for a second phase of injection was obviated. Optimization involved varying only those parameters associated with a single phase of the trajectory, v_{jet}, and the rates of coil acceleration and deceleration, with the latter defined by the cut-off frequencies of two first order low pass filters applied to the acceleration and deceleration phases of the injection (Figure 1).

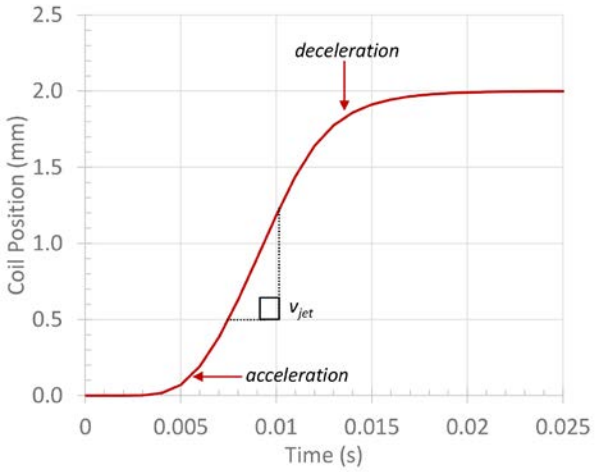

Figure 1: Typical coil trajectory for an injection of 20 µL of fluid. The maximum slope is proportional to v_{jet} which in this case is 100 m/s. This trajectory is filtered with 75 Hz and 50 Hz acceleration and deceleration low pass filters respectively.

Ex vivo mouse skin, collected through the MIT Tissue Harvest Program was used to optimize the parameters required for repeatable intradermal delivery of HBsAg. Tissue plugs, obtained from *ex vivo* BALB/c mouse skin using a 12 mm diameter punch, were seated in a 24 well tissue culture plate containing Whatmann 3MM filter paper discs soaked in physiological saline. Each was injected with a requested volume of 20 µL of a 1:20 dilution of red tissue marking dye (Polysciences, Inc.) in HEPES-NaCl buffer at velocities of 30, 60, 80, 100, and 120 m/s. Acceleration and deceleration rates of the coil were limited by filtering the acceleration and deceleration phases of the trajectory to 75 Hz and 50 Hz, respectively. In a second series of experiments, tissue samples were injected with 20 µL volumes at a velocity of 100 m/s, while the coil deceleration cut-off frequency was varied from 50 Hz through 150 Hz in 25 Hz increments, and the coil acceleration frequency was maintained at 75 Hz.

Post injection tissue plugs were trimmed, medially sectioned through the injection site, splayed injection plane up, and photographed. Tissue plugs from each experimental group were either embedded in optimal cutting temperature compound (Tissue-Tek® O.C.T. Compound, Sakura Finetek®) and 10 µm thick sections collected using a cryostat microtome (Vibratome) or embedded in paraffin and 5 µm thick sections collected by microtome. Sections were stained with Mayer's Hematoxylin (Dako Agilent Pathology Solutions), coverslipped, imaged using an upright microscope (Eclipse E800, Nikon Inc.), and photographed with a SLR camera (EOS1-Ds1, Canon Inc.).

Recovery of antigen for determination of antibody binding

Tissue plugs, obtained from *ex vivo* BALB/c mouse skin injected with HBsAg using 3 mm biopsy punches, were placed in 1 mL to 2 mL of homogenization buffer [34Ahtikoski2004] and homogenized on ice using ten 5-second pulses of a PT1200C polytron (Kinematica AG) at maximum power. The homogenates were briefly centrifuged and each supernatant aliquoted over five 1.5 mL Eppendorf tubes. Total protein concentration was determined using a detergent compatible colorimetric assay

based on the Lowry method (DC protein assay, Bio-Rad Life Science). Aliquots were stored at -20 °C until ready for use.

Immunization of animals with HBsAg

Seventeen female BALB/c mice (Charles River Laboratory), ages six- to eight-weeks, were used to evaluate the induction of an immune response to HBsAg (Meridian Life Sciences). The mice were littermates and/or closely age matched. All mice were housed under specific pathogen-free conditions and were acclimated to the animal facility for one week prior to immunization.

On the day of the experiment, the animals were weighed and anesthetized using 3% isoflurane in balanced oxygen delivered using a rodent anaesthetic machine (Impac 6). While anaesthetized, mice were given ear tags for identification, 50 µL - 100 µL of blood was collected via retro-orbital bleeding (pre-immune serum), and the area to be injected cleansed using Betadine Scrub followed by 70 % Et0H. Anaesthesia was maintained during the course of the injections by administration of 2.5 % - 3 % isoflurane in balanced oxygen using a modified nose cone.

Groups of four mice were immunized at a time with HEPES buffer adsorbed to aluminum hydroxide gel (Alhydrogel [$Al(OH)_3$] referred to as alum, Sigma) or alum-adsorbed HBsAg at a concentration of 0.1 g/L. Adsorption of antigen to alum was determined by measuring the protein concentration in the supernatant by the Bradford method [35Bradford1976] after centrifugation at 2000 rpm for 3 minutes. The first group of four mice were given intradermal (ID) abdominal injections of alum-adsorbed HEPES buffer using the JI (negative control). A second and third group of four mice were given intradermal abdominal injections of alum-adsorbed HBsAg using the JI and a 27G NS respectively. A final group of four mice were injected subcutaneously at the base of the tail with alum-adsorbed HBsAg using a 27G NS (positive control). A single mouse was given a subcutaneous (SC) injection of alum-adsorbed HEPES buffer at the base of the tail. Administration required that the JI be placed against the skin and actuated. Fluid pressures developed during delivery were ~5 MPa, based on injection depths observed given preliminary studies using *ex vivo* tissue.

The mice were immunized at day 0 and then again at day 14 and day 28, with blood being collected via retro-orbital sinus bleeds immediately prior to each immunization or boost. Prior to euthanization at day 47, a single mouse was injected with a 1:20 dilution of filter-sterilized red tissue marking dye using the JI and the site biopsied immediately post euthanization in order to assess penetration depth by histology.

Animals were euthanized using $C0_2$ and blood collected via cardiac puncture. Serum was isolated and stored in 50 µL aliquots at -20 °C. All sera were assayed by indirect ELISA for antibodies to HBsAg (HBs antibodies). Mice were monitored tri-weekly post injection for any signs of pain or distress. Immunization sites were examined for evidence of lesions such as swelling, abscess or fistula formation, infection, or ulceration throughout the course of the experiment.

ELISAs to quantify soluble HBsAg and serum antibody levels

Given that Ag coating time and substrate incubation time could each affect the resultant absorbance these parameters were held constant in all ELISAs. Checkerboard

titration [36Crowthers2001] was used to optimize the coating, secondary, and tertiary reactant conditions.

Soluble HBsAg alone or alum-adsorbed HBsAg ejected into tubes and total protein extracts recovered from HBsAg- or alum-absorbed HBsAg-injected into ex vivo tissue were quantified by direct sandwich ELISA. CAPTURE monoclonal antibodies (10 mg/L CAPTURE mAb, Meridian Life Science) in phosphate buffered saline (BupH™ PBS, Pierce) were bound to ninety-six-well flat-bottom microtiter plates (Nunc MaxiSorp®, VWR) at 4 °C overnight. Unbound antibody (Ab) was removed by washing with BupH™ PBS and each well blocked in Starting Block™ T20 (SB, Pierce) for fifteen minutes at room temperature. After 5 more washes with BupH™ PBS, excess buffer was removed and 50 µL serial dilutions of 1) reference HBsAg (for standard curve), 2) ejected antigen , or 3) total protein extract from antigen- or buffer-injected *ex vivo* tissue were added to appropriate wells. Plates were sealed, incubated overnight at 4 °C, washed and blocked as above after which 50 µL of Hepatitis B antibody conjugated to horseradish peroxidase (HRP-DETECTION mAb, Meridian Life Science; EZ Link, Pierce) was added to each well at a final concentration of 50 µg/L or 200 µg/L. Plates were sealed and incubated for two hours at room temperature. Unbound antibody was removed by washing, the plates were blocked again, and 50 µL of 3,3',5,5'-tetramethylbenzidine (TMB, Pierce) was added to each well. Following a brief (30 s) centrifugation, the plates were incubated for 30 minutes to maximize color detection. The reaction was stopped by adding 50 µL of 2 mol/L sulfuric acid, and the absorbance values read using a Molecular Devices SpectraMax Plus384 spectrophotometer at 450 nm. A standard curve was generated from serial diluted HBsAg samples and used to determine antigen concentrations in protein extracts.

Serum antibody levels were quantified using indirect ELISA which was performed under similar conditions to those noted above, with the following modifications: HBsAg was bound to each well of ninety-six well plates; 1:50000, 1:100000, and 1:200000 dilutions of non-conjugated DETECTION mAb were added to appropriate wells to generate standard curves; 1:100 dilutions of serum in SB were added to the remaining wells. Plates were washed to remove unbound antibody and a 1:10000 dilution of secondary antibody conjugated to HRP (GAM-HRP) was added to all wells. Following incubation and washing, TMB was added to all wells, the reaction stopped and absorbance read at 450 nm. Anti-HBsAg antibody was affinity purified using aminolink plus gel spin columns and reagents (ThermoFisher Scientific).

Relative titers were determined by equating the absorbance values (a relative measure of the amount of antibody bound) of serially diluted serum from mice immunized with HBsAg to those obtained from serially dilutions of a known concentration of standard antibody (DETECTION mAb with specificity for HBsAg) according to [37Cooper2000]. Absorbance was determined following incubation with the HRP-conjugated secondary antibody and addition of TMB as above.

Analysis of variance.

Single factor ANOVA, two factor ANOVA with replication, and Tukey Kramer analyses were used to assess differences in the treatment and/or mode of delivery. $P \leq 0.05$ was considered a statistically significant difference.

Results and Discussion

Effect of injection Parameters on delivery to ex vivo tissue

Prior to injection of antigen into mice, delivery of tissue marking dye or HBsAg containing tissue marking dye to *ex vivo* tissue was evaluated in order to optimize the parameters required for intradermal jet injection. As anticipated [26][38Baxter2005][39Hemond2011], increasing the jet velocity while maintaining constant rates of acceleration and deceleration resulted in an increased depth of penetration up to a maximum of approximately 0.75 mm, which was observed at a v_{jet} of 100 m/s (Figure 2A). At velocities greater than 80 m/s, more than 75% of the ejected volume was delivered to the tissue. Substantial variability in injection depth was observed at and beyond a set velocity of 120 m/s as in many cases the jet penetrated the tissue, which on average was 2.0 mm ± 0.6 mm thick.

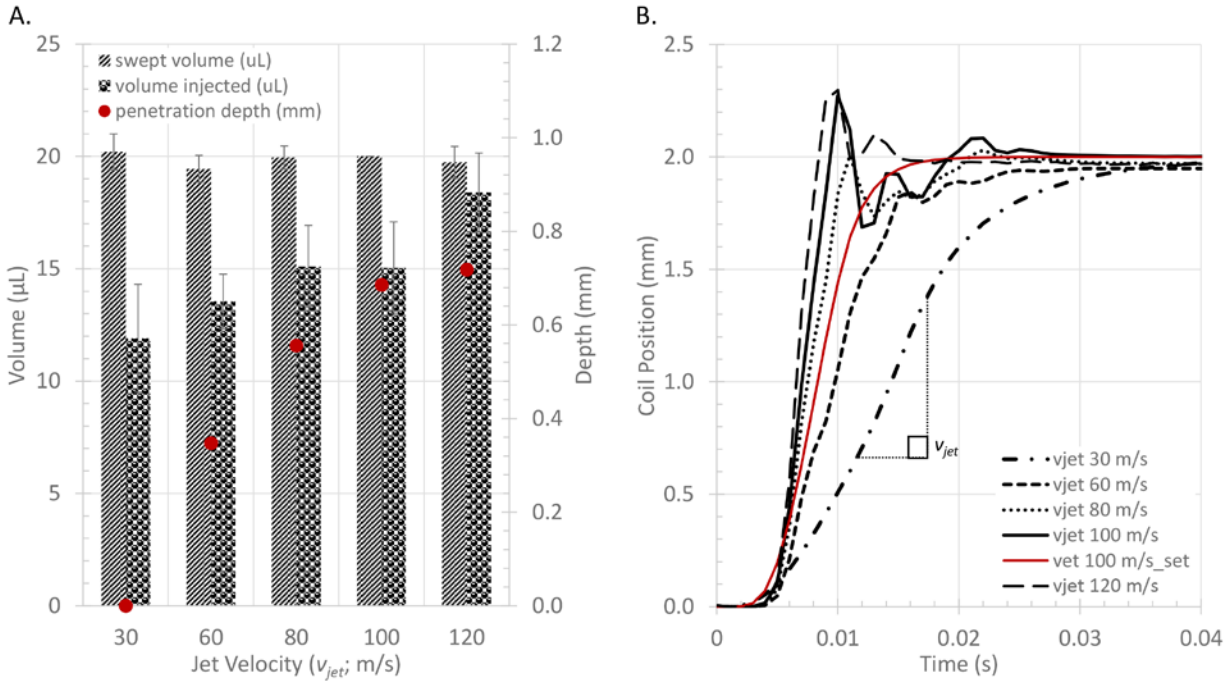

Figure 2: Effect of v_{jet} on delivery. **A.** Plot showing penetration depth, and volume swept and delivered as a function of v_{jet}. The swept volume is plotted along with the actual volume injected into the tissue wherein the latter is determined gravimetrically. Each bar with error bars represents the mean and standard deviation of 10 to 50 injections. **B.** Plot showing typical acceleration of the coil to requested velocities (v_{jet}) of 30, 60, 80, 100 and 120 m/s with a tissue load. Cutoff frequencies of 75 Hz and 50 Hz were used to control acceleration and deceleration respectively of the injector. A single plot (red line) depicts the corresponding requested trajectory for delivery of a volume of 20 µL at a v_{jet} of 100 m/s in the absence of a tissue load.

The overshoot evident in the coil position response shown in Figure 2B is a consequence of the mass of the coil and piston resonating with the mechanical admittance of the piston tip, ampoule, and fluid load [40Williams2012][41Williams2015]. The force required to accelerate the fluid to high jet speeds results in considerable compression of the piston tip in comparison to the distance traveled. Yet the total volumes ejected by the injector and delivered to the tissue remained close to the target volume of 20 µL.

Increasing the deceleration cut-off frequency while maintaining constant v_{jet} and acceleration rate (Figure 3) effectively increased the depth of penetration. While v_{jet} remained relatively constant (~120 m/s), it was sustained for a longer period, and faster deceleration rates resulted in greater overshoot and more resonance as the coil and piston were forced to rebound more quickly and stop more abruptly (Figure 3A). The volume of drug delivered to the tissue decreased, a consequence of the drug being driven through the tissue. Thus, acceleration and deceleration cutoff frequencies of 75 Hz proved optimal, and were used for subsequent experiments.

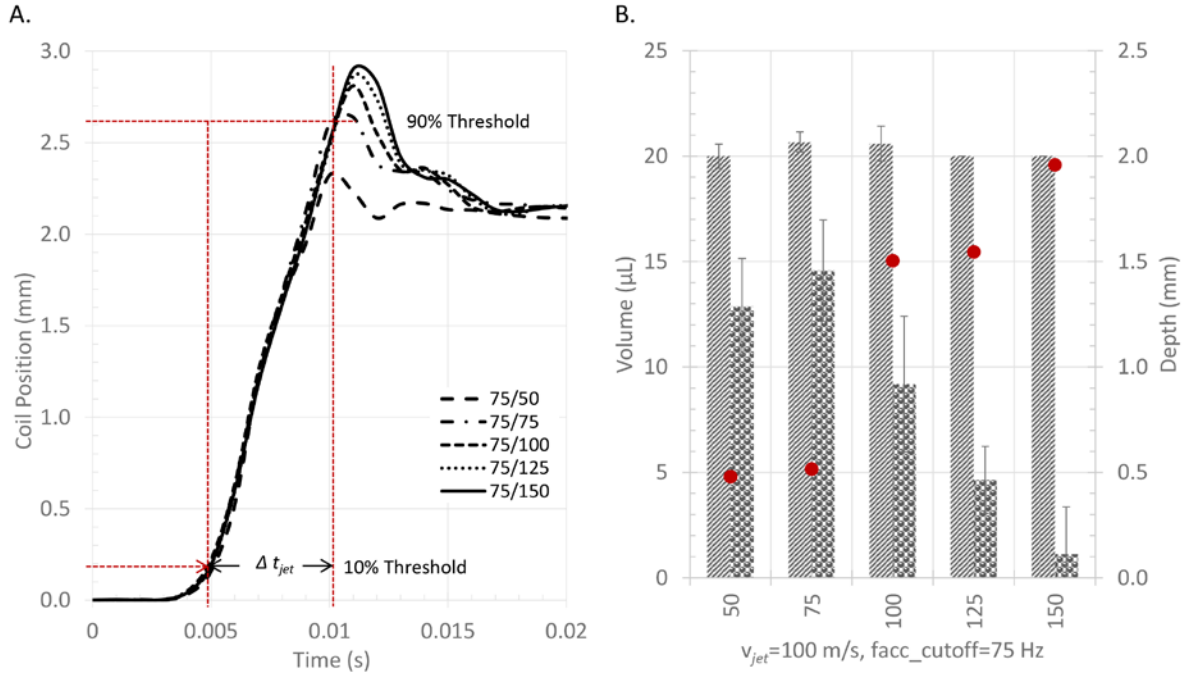

Figure 3: Effect of deceleration rate on injection performance. **A.** Plot of coil position as a function of time for injections wherein the rate of deceleration was varied using a low pass filter with cutoff frequencies of 50, 75, 100, 125, and 150 Hz; v_{jet} = 100 m/s and a cutoff frequency of 75 Hz was applied to the acceleration, n = 5 repeats at each parameter value. The time required for the response to rise from 10% to 90% of the final value was determined, the velocity calculated (slope*[A_{piston}/A_{nozzle}]), and found to be comparable for all injections. **B.** Plot showing penetration depth and volume delivered as a function of the cutoff frequency of the filter used for deceleration. Both the swept volume and volume injected into tissue as determined gravimetrically are shown. Deceleration frequencies of 100 Hz and above resulted in complete penetration of the tissue.

Effect of adjuvant on antigen stability

The amount of antigen required to elicit an antibody response in laboratory animals (*i.e.* the window of immunogenicity) varies depending on the antigen and species; tolerance can be induced with too much or too little. As such, antigens are often injected with an adjuvant thereby permitting the use of smaller quantities of antigen while assuring a high quality, high quantity, memory-enhanced antibody response [42Hanly1994]. Aluminium adjuvants are widely used in both human (e.g. Engerix B, a non-infectious recombinant DNA Hepatitis B vaccine expressed in *S. cerevisiae*) and veterinary vaccines (For review, see [43Lindblad2004]). While weaker adjuvants than emulsion adjuvants, these adjuvants exhibit a mild inflammatory reaction, are safe, generate memory, and are the only agent approved for use in human vaccines.

Mechanisms to explain improved immunogenicity associated with the use of these salts include a particulate nature and size (<10 µm) that permits phagocytosis, direct stimulation of the immune system through enhanced Th2 cytokine production, greater exposure to antigen presenting cells as they are repository in nature, and decreased thermal stability [43Lindblad2004][44Jones2005][45Gupta1998]. Of these mechanisms, the last two were of particular interest given the delivery mechanisms being compared and the possibility for further destabilization of a potentially compromised antigen when exposed to the high pressures used for jet injection.

The effect of adsorption to Alhydrogel on the integrity of the antigen, to the extent that HBsAg is a conformational antigen [46Cregg1987][47Tollais1985], was evaluated indirectly by assessing its ability to bind HBs antibodies post ejection. A constant volume of HBsAg alone or alum-adsorbed HBsAg was ejected into test tubes using the JI and antigen-antibody binding compared with that observed for antigen ejected using a 27G NS and the Medi-Jector VISION (M-J VISION), a spring-actuated jet injector. The exclusion of adjuvant provided a means to evaluate whether inclusion of adjuvant alone altered binding affinity. As shown in Figure 4, neither adjuvant alone nor ejection in the presence or absence of adjuvant appeared to alter antigen binding as determined indirectly by absorbance.

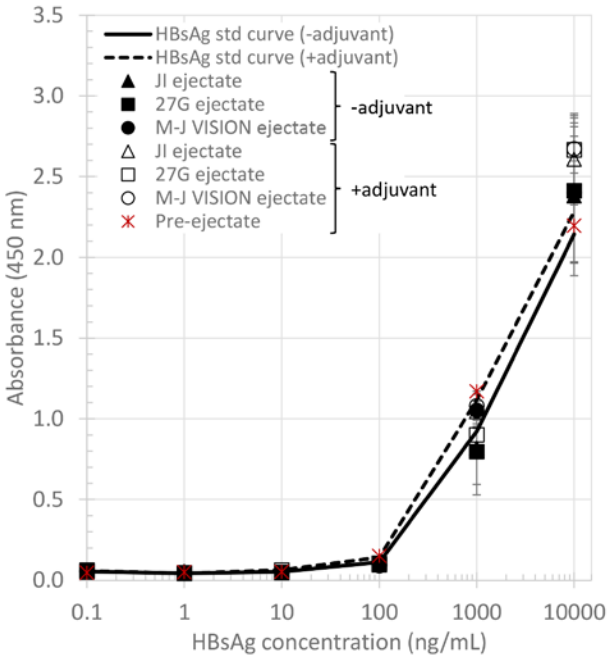

Figure 4: Effect of ejection and inclusion of adjuvant on the ability of HBsAg to bind HBs antibodies. HBsAg (0.1 g/L), equilibrated in an equal volume of HEPES buffer or HEPES-equilibrated $Al(0H)_3$ buffer, ejected using the JI, 27G NS, or M-J VISION (a spring-actuated injector) was bound to CAPTURE Ab and differences in the amount of antigen bound determined using a constant concentration of HRP-conjugated DETECTION Ab. CAPTURE Ab and DETECTION Ab were used at concentrations of 10 mg/L and 0.2 mg/L respectively. Comparable results (not shown) were obtained using a DETECTION Ab concentration of 50 µg/L. Plots displaying antigen binding using a two-site enzyme immunoassay. *Vol* = 20 µL, v_{jet} = 100 m/s, acceleration and deceleration of 75 Hz.

Absorbance values obtained for each treatment (no ejection and ejection using one of the JI, 27G NS, or M-J VISION) (*P-value* ≥0.404) and each group (plus or minus adjuvant) (*P-value* ≥0.427) at each of six independent concentrations tested were

comparable (*P-value* > 0.05) indicating that, within the boundaries of this experiment, there is no significant difference in antibody binding. Non-specific binding of HBsAg to non-specific antibody or HRP-conjugated antibody, either GAM-HRP or an unrelated secondary HRP-antibody, as observed by [48Omata1980] was not detected (data not shown).

Injection of antigen into ex vivo tissue

When delivering fluid using a needle and syringe, the fluid is deposited as a bolus directly to the desired target tissue. With a jet injector, once the fluid exits the nozzle it has to penetrate one or more layers of tissue prior to reaching the desired target with dispersion being dependent on the material properties of the tissue through which the jet streams. Given the target tissue is the dermis, an anisotropic and inhomogeneous tissue, the effect of the inclusion of aluminium salt (a colloid suspension with a density of 2.42 g/cm^3) on the parameters required to deliver antigen to the dermis was re-assessed, as was the dispersion pattern of the antigen in the tissue.

Fixed volumes of HBsAg and alum-adsorbed HBsAg were injected into *ex vivo* tissue using the JI or a conventional 27G NS. Tissue plugs collected from the site of injection were either processed individually for histological staining in order to confirm delivery to the dermal tissue or total protein was extracted from each plug, quantified to ensure that comparable amounts were loaded into downstream analyses, and relative binding activity assayed (Figure 5). The invariant pressure profile associated with the M-J VISION, designed to deliver drug to the subcutaneous layer, consistently propelled drug through the tissue thereby precluding its further use in these studies.

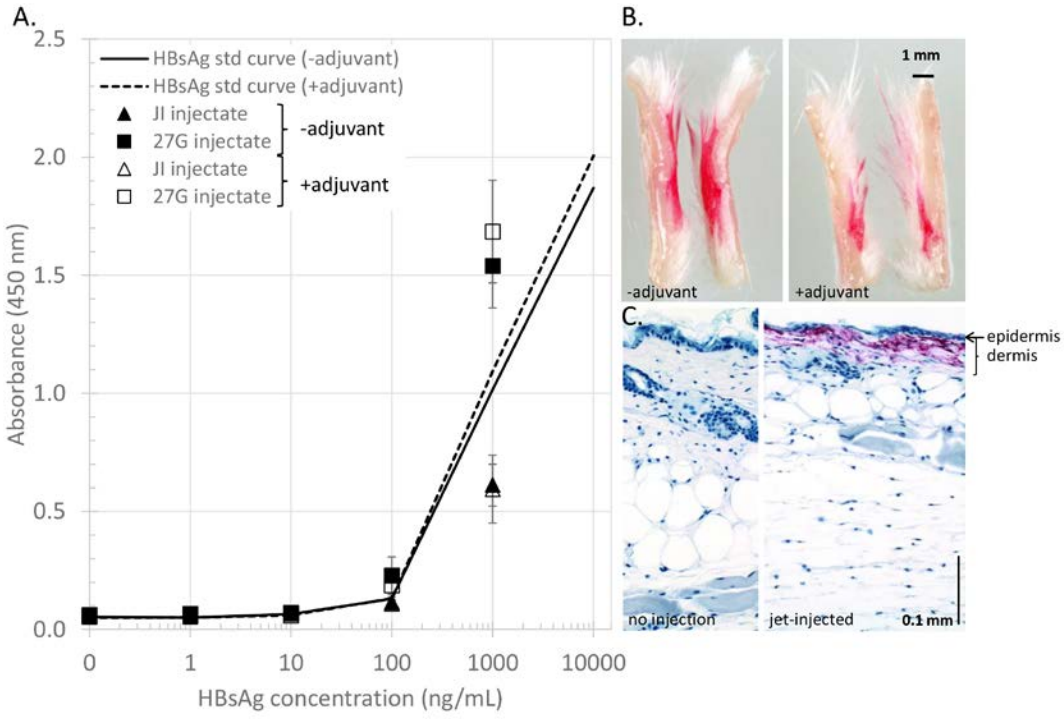

Figure 5: Delivery and binding of antigen in total protein extracts from *ex vivo* tissue injected with 2.0 µg of HBsAg or alum-adsorbed HBsAg. **A.** Plot showing binding as determined by absorbance for serial dilutions of HBsAg-containing tissue homogenates. Total protein extracted from 2 mm tissue plugs from sites injected using either the JI or a 27G NS was quantified by the Lowry method. A 50 µL volume of

serial dilutions of total protein extract was then loaded into each well of a 96 well plate previously coated with CAPTURE Ab for detection of binding by sandwich ELISA. **B.** Representative delivery of a mixture of dye and antigen ± adjuvant to *ex vivo* tissue. **C.** 5 µm sections of *ex vivo* tissue injected with dye and counterstained with Hematoxylin; no injection serves as a control.

Histological analysis showed that HBsAg and alum-adsorbed HBsAg were each delivered to the dermis using the JI with no obvious difference in dispersion pattern. Comparable analysis was not done for skin injected using the Mantoux method.
No difference in binding activity was observed for HBsAg and alum-adsorbed HBsAg at each of five concentrations tested in tissue homogenates collected from JI-injected sites alone or 27G NS-injected sites alone (within groups) when indirectly indexed by absorbance values. However, between groups, a significant difference in the amount of antibody bound was observed with absorbance values being higher for antigen (HBsAg or alum-adsorbed HBsAg) recovered from 27G NS-injected sites (*P-value* = 6.6E-03 for 100 µg/L and 2.7E-05 for 1000 µg/L). Variation in both the volume of antigen delivered and the recovery of antigen in tissue homogenates resulting from differential antigen acquisition during biopsy collection due to differential dispersion could account for this difference. On average, 24 µL ± 3.4 µL of antigen was injected into *ex vivo* tissue using the 27G NS as compared to 14.1 µL ± 2.2 µL using the JI.

JI-injected HBsAg is immunogenic in mice

As shown in Figure 6, pre-immune sera did not react with HBsAg nor did the serum collected from animals vaccinated with alum-adsorbed HEPES buffer. However, serum from animals vaccinated with alum-adsorbed HBsAg showed specific binding to HBsAg irrespective of the delivery mode or location. Moreover, a statistically significant increase in the amount of antibody bound at different time points in serum collected from HBsAg-injected mice was detected with an apparent maximum observed at day 47, the final bleed out. No binding was observed in the no antibody and mouse IgG negative controls (data not shown).

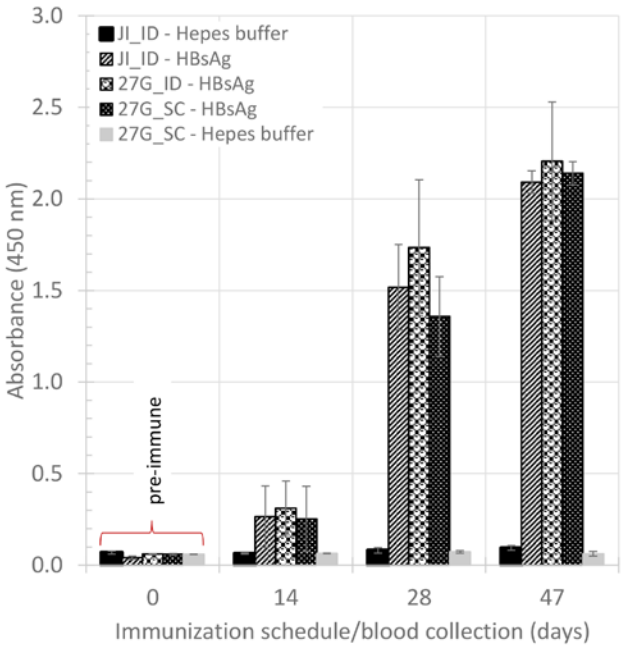

Figure 6: Immunogenicity of HBsAg in mice as determined by indirect ELISA. Mice were vaccinated three times on days 0, 14, and 28 with blood draws prior to each vaccination and 19 days after the final boost. Serum samples were tested at 1:100 dilutions against HBsAg. Optimal concentrations of mouse antisera and anti-mouse conjugate were determined by checkerboard titration [22]. The results show the mean absorbance and standard deviation for n=8 tests (4 x 2).

Comparison of the average absorbance values for each time point suggested no difference between the different delivery modes (JI vs 27G NS) and location (ID vs SC) (*P-value* $\geq$ 0.449). However, absorbance values at day 47 are approaching a plateau where the antigen is saturated. As such, determination of relative titer for comparison of delivery modes using these values is unreliable.

A more accurate comparison of the immune response elicited using the JI with that elicited using a 27G NS can be realized by estimating the HBs antibody titers on further dilution of the serum. Antibody titer for each delivery mode and location was determined by assaying serial dilutions of pooled serum from each group collected 19 days after the final immunization (day 47)(Figure 7). While there are several methods by which titers can be calculated (for example, [49Frey1998; 50Miura2008]), in this study relative titer (*1/x***z*, where *x* = concentration [g/L] and *z* = serum dilution) was determined by equating the relative absorbance which represents a measure of the antibody bound (*y*) obtained from serial dilutions of the DETECTION mAb (*z*; known standard) with that obtained from serial dilutions of antiserum (*1/x*) according to [37Cooper2000]. Because the curves shown in Figure 7A are parallel, any point within the linear portion of the curves can be taken for comparison of samples [36Crowthers2001][37Cooper2000]. As serial dilutions of a known concentration of the DETECTION mAb (not shown) were assayed along with our unknowns, absolute values could be rendered from relative absorbance measures (Figure 7B).

A.

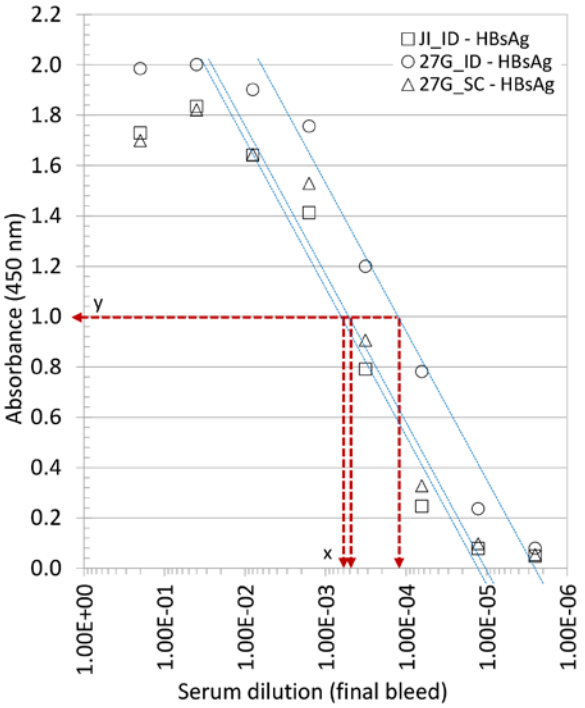

B.

INJECTION MODE	HBsAg INJECTED (µg)	SPECIFIC TITER (Ab. dil * std [Ab])
JI_ID injection	1.97	0.456 (±0.087)
27G_SC injection	2.38	0.529 (±0.104)
27G_ID injection	4.83	2.042 (±0.571)

Figure 7: Anti-HBsAg titers at day 47 for mice immunized with three doses of alum-adsorbed HBsAg (one primary dose and 2 boosters) using a JI or 27G NS. Injections using the JI were ID while those given using a 27G NS were ID or SC. A. Serum titration curves for determination of antibody titer with or without a standard curve. In higher dilutions of sera, the endpoint titers are 2x lower for sera collected from JET INJECTOR/ID and 27G/SC injected mice if the cutoff established for the 1:100 dilution of the negative controls is used to determine the endpoint. B. Titer as determined using a standard curve.

No significant difference was detected between the titers for mice vaccinated intradermally using the JI or subcutaneously using a 27G NS (*P-value* = 0.0877); the immune response elicited was comparable (Figure 7B). However, both exhibited serum antibody titers significantly lower than the titer detected in serum from mice injected intradermally using a 27G NS (*P-value* = 3.9E-13 and Tukey-Kramer analysis). This difference in titer reflects a difference in the concentration of antigen injected at each time point as determined gravimetrically. Animals vaccinated by intradermal injection using a 27G NS received on average 4.83 µg of alum-adjuvanted HBsAg as compared to 2.38 µg and 1.97 µg for mice given SC injections using a 27G NS or ID injections using the JI respectively. While the intent was to deliver two 2 µg injections (or a total of 40 µL) to the dermis, difficulties inherent in accurately loading a needle and syringe with a 20 µL volume together with administration using the Mantoux method contributed to variability in volume delivered using the 27G NS (48.3 µL ± 6.9 µL). While loading and the desired ejection volume were controlled using the JI, variability in delivered volume was observed. As evidenced in Figures 2A and 3A, increasing the velocity and the cut off frequency for deceleration resulted in considerable overshoot in the coil position, an outcome attributed primarily to exciting the resonance of the system due to the sharp voltage pulse. Given that volume delivered is quite small (20 µL), the deformation of the piston tip and shaft with the applied force is large relative to the distance traveled with the resultant ringing making estimation of the volume by the potentiometer less accurate.

Throughout the course of this study, the animals were monitored for signs of pain or distress and injection sites monitored for evidence of erythema, swelling, bruising, or infection. While minor bleeding at injections sites was observed in some animals using JI or 27G NS immediately post injection, no adverse events were recorded.

Conclusion

ID vaccination exploits the ability of dermal keratinocytes and Langerhan's cells (LCs) to stimulate naïve resting T-cells for antigen-specific CD4+ and CD8+ T-cell responses. Mice vaccinated with a comparable amount of alum-adsorbed HBsAg by intradermal injection using the JI or subcutaneous injection using a 27G NS exhibited non-inferior titers; the immune response in these animals was comparable. Differences in titer observed between mice vaccinated intradermally using either the JI or a 27G NS reflect differences in the volume of antigen delivered to the target.

Consistent delivery of a 20 µL volume to the dermis by the Mantoux method using a 27G NS proved difficult, although the variability might easily be remedied by implementation of an investigational adaptor as developed by West Pharma and tested by PATH [25Jarrahian2012]. Much of the volume variability detected in injections using the JI could be attributed to the effects of the compliance of the commercially available ampoule used in this study, which is designed for injection volumes ten-fold higher than those conducted here. Repeatability of the volume delivered using the JI can be improved by reducing the compliance of the system. Replacement of the ampoule and piston with stiffer counterparts should reduce some of the ringing observed in the coil displacement time profiles. As discussed in [40], these measures should permit more accurate estimation of fluid volume by the potentiometer and reduce overshoot, thereby providing tighter control over jet speed during the course of the injection. Tighter control of jet velocity should in turn provide higher consistency of injection depth.

While vaccinated animals displayed evidence of HBs antibodies in response to intradermal delivery of antigen using the JI, the effectiveness of the antibodies generated against an HBV challenge should be evaluated in future studies.

Application of this technology to a more general audience would benefit from inclusion of a force sensor to ensure that the force with which the JI is applied to the skin could be controlled [51Demas]. Given the variability in the mechanical properties of skin with age, skin type, hydration level, body location, and among individuals, some measure of the mechanical properties of the tissue prior to an injection may help to inform the parameters required to deliver drug to the desired target.

Acknowledgements

The authors would like to thank the Division of Comparative Medicine for their guidance and training.

References

[1] C. DeBenedictis, S. Joubeh, G. Zhang, M. Barria, and R.F. Ghohestani, Immune function of the skin, Clin. Derm. 19 (2001) 573-585.

[2] B. Malissen, S. Tamoutounour, and S. Henri, The origins and functions of dendritic cells and macrophages in the skin, Nat. Rev. Immunol. 14(6) (2014) 417-428.

[3] D. Zehrung, C. Jarrahian, and A. Wales, Intradermal delivery for vaccine dose sparing: Overview of current issues, Vaccine 31 (2013) 3392-3395.
[4] N. Romani, V. Flacher, C.H. Tripp, F. Sparber, S. Ebner, and P. Stoitzner, Targeting skin dendritic cells to improve intradermal vaccination, Curr. Top. Microbiol. Immunol. 351 (2012) 113-138.
[5] S.M. Bal, Z. Ding, E. van Riet, W. Jiskoot, and J.A. Bouwstra, Advances in transcutaneous vaccine delivery: do all ways lead to Rome?, J. Control Release 148 (2010) 266-282.
[6] B.G. Weniger and M.J. Papania, Alternative vaccine delivery methods, in: S.A. Plotkin, W.A. Orenstein, P.A. Offict, (Eds.), Vaccines, 6th edition, Elsevier/Saunders, Philadelphia; 2013, p.p. 1200-1231.
[7] Lambert, P.H. and Laurent, P.E. Intradermal vaccine delivery: Will new delivery systems transform vaccine administration? Vaccine 26 (2011) 3197-3208.
[8] N.C. Hogan, A.J. Taberner, L.A. Jones, and I.W. Hunter, Needle-free delivery of macromolecules through the skin using controllable jet injectors, Exp. Opin. Drug Delivery 12(10) (2015) 1637-1648.
[9] Y–C. Kim, J-H. Park, and M.R. Prausnitz, Microneedles for drug and vaccine delivery, Adv. Drug Del. Rev. 64 (2012) 1547-1568.
[10] C.H. Saroja, P.K. Lakshmi, and S. Bhaskaran, Recent trends in vaccine delivery systems. A review, International J. Pharm. Invest. 1(2) (2011) 64-74.
[11] D. Kristensen, D. Chen, and R. Cummings, Vaccine stabilization: Research, commercialization, and potential impact, Vaccine 29 (2011) 7122-7124.
[12] L. McAllister, J. Anderson, K. Werth, I. Cho, K. Copeland, N. Le Carn, D. Plant, P.M. Mendelman, and D.K. Cobb, Needle-free jet injection for administration of influenza vaccine: a randomized non-inferiority trial. The Lancet 384 (2014) 674-681.
[13] M.J. Sarno, E. Blasé, N. Galindo, N, R. Raminrez, C.L. Schirmer, and D.F. Trujillo-Juarez, Clinical immunogenicity of measles, mumps and rubella vaccine delivered by the Injex jet injector: comparison with standard syringe injection, Pediatr. Infect. Dis. J. 19(9) (2000) 839-842.
[14] I.H.J. Ploemen, H.J.H.B. Hirschberg, H. Kraan, A. Zeltner, S. van Kuijk, D.P.K. Landveld, D.P.K., M. Royals, G.F.A. Kersten, and J-P. Amorij, Minipigs as an animal model for dermal vaccine delivery, Comparative Medicine 64(1) (2014) 50-54.
[15] J. Williams, L. Fox-Leyva, C. Christensen, D. Fisher, E. Schlicting, M. Snowball, S. Negus, J. Mayers, R. Koller, and R. Stout, Hepatitis A vaccine administration: comparison between jet-injector and needle injection, Vaccine 18 (2000) 1939-1943.
[16] G.F. Jones, V. Rapp-Gabrielson, R. Wilke, E.L. Thacker, J. Thacker, L. Gergen, D. Sweeney, and T. Wasmoen, Intradermal vaccination for Mycoplasma hyopneumoniae. J. Swine Health Prod. 13(1) (2005) 19-27.
[17] R.A. Gramzinski, C.L. Brazolot Millan, N. Obaldia, S.L. Hoffman, and H.L. Davis, Immune response to Hepatitis B DNA vaccine in Aotus monkeys: a comparison of vaccine formulation, route, and method of administration, Mol. Med. 4 (1998) 109-118.
[18] A.J. Mohammed, S. AlAlwaidy, S. Bawikar, P.J. Kurup, M.P.H.Emadaldin Elamir, M.M.A. Shaban, S.M. Sharif, H.G.A.M. van der Avoort, M.A. Pallansch, P.

Malankar, A. Burton, M. Sreevatsava, and R.W. Sutter, Fractional doses of inactivated poliovirus vaccine in Oman, N. Engl. J. Med. 362(25) (2010) 2351-2359.
[19] L. Gergen, B. Eddy, K. Menassa, C. McGregor, and T. Wasmoen, Intramuscular and intradermal vaccination of swine for swine influenza virus and Mycoplasma hyopneumoniae using a needle-free device, Allen D. Leman Swine Conference (2002). Retrieved from the University of Minnesota Digital Conservancy, http://hdl.handle.net/11299/160450.
[20] B.S. Graham, M.E. Enama, M.C. Nason, DNA vaccine delivered by a needle-free injection device improves potency of priming for antibody and CD8+ T-cell responses after rAd5 boost in a randomized clinical trial, PLOS ONE 8(4) (2013) 1-11.
[21] J.C. Aguiar, R.C. Hedstrom, W.O. Rogers, Y. Charoenvit, J.B. Sacci, D.E. Lanar, V.F. Majam, R.R. Stout, and S.L. Hoffman, Enhancement of the immune response in rabbits to a malaria DNA vaccine by immunization with a needle-free jet device, Vaccine 20 (2002) 275-280.
[22] S. Resik, A. Tejeda, O. Mach, C. Sein, N. Molodeck, C. Jarrahian, L. Saganic, D. Zehrung, M. Fonseca, M. Diaz, N. Alemany, G. Garcia, L.H. Hung, Y. Martinez, and R.W. Sutter, Needle-free jet injector intradermal delivery of fractional dose inactivated poliovirus vaccine: Association between injection quality and immunogenicity, Vaccine 33 (2015) 5873-5877.
[23] S. Kwilas, J.M. Kishimori, M. Josleyn, K. Jerke, J. Ballantyne, M. Royals, and J.W. Hooper, A hantavirus pulmonary syndrome (HPS) DNA vaccine delivered using a spring-powered jet injector elicits a potent neutralizing antibody response in rabbits and nonhuman primates, Curr. Gene Ther. 14(3) (2014) 200-210.
[24] C. Cappello, M. Wixey, and J.W. Bingham, Needle-free intradermal injection device, US 2013/0150820 A1 published 13 June 2013.
[25] C. Jarrahian, D. Zehrung, E. Saxon, E. Griswold, and L. Klaff, Clinical performance and safety of the ID adapter, a prototype intradermal delivery technology for vaccines, drugs, and diagnostic tests, Procedia. Vaccinol. 6 (2012) 125-133.
[26] J.C. Stachowiak, T.H. Li, A. Arora, S. Mitragotri, and D.A. Fletcher, Dynamic control of needle-free jet injection. J. Control Release 135 (2009) 104-112.
[27] A.J. Taberner, N.C. Hogan, and I.W. Hunter, Needle-free jet injection using real-time controlled linear Lorentz-force actuators, Med. Eng. Phys. 34 (2012) 1228-1235.
[28] A.D. Kosinska, E. Zhang, M. Lu, and M. Roggendorf, Therapeutic vaccination in chronic hepatits B: preclinical studies in the woodchuck, Hepat. Res. Treat. 817580 (2010) 1-17.
[29] W.H. Gerlich, Medical virology of hepatitis B: how it began and where it is now, Virology Journal 10 (2013) 239. doi:10.1186/1743-422X-10-239.
[30] S. Leonardi, M. Miraglia del Guidice, L. Spicuzza, M. Spina, and M. La Rosa, Hepatitis B vaccine administered by intradermal route in patients with celiac disease unresponsive to the intramuscular vaccination schedule: a pilot study, Am. J. Gastroenterol. 105(9)2117-2119. DOI:10.1038/ajg.2010.195.
[31] F. Fabrizi, V. Dixit, P. Messa, and P. Martin, Intradermal vs intramuscular vaccine against hepatitis B infection in dialysis patients: a meta-analysis of randomized trials, J. Viral Hepatitis 18 (2011) 730-737.

[32] B.D. Hemond, D.M. Wendell, N.C. Hogan, A.J. Taberner, and I.W. Hunter, A Lorentz-force actuated autoloading needle-free injector, 28th IEEE EMBC Annual International Conference 2006: 679-682.
[33] J.H. Chang, Needle-free interstitial fluid acquisition using a Lorentz-force actuated jet injector (PhD thesis), Dept. Mechanical Engineering, MIT 2014.
[34] A.M. Ahtikoski, E-M. Riso, S.O.A. Koskinen, J. Risteli, and T.E.S. Takala, Regulation of type IV collagen gene expression and degradation is fast and slow muscles during dexamethasone treatment and exercise, Pflugers Arch. – Eur. J. Physiol. 448 (2004) 123-130.
[35] M.M. Bradford, A rapid and sensitive method for the quantitation of microgram quantities of protein utilizing the principle of protein-dye binding, Anal. Biochem. 72 (1976) 248-254.
[36] J.R. Crowthers, Methods in Molecular Biology, The ELISA Guidebook 149. Humana Press 2001.
[37] H.M. Cooper and Y. Paterson, Determination of specific antibody titer and isotype, Chapter 11. Current Protocols in Molecular Biology (2000) 11.17.1-11.17.13.
[38] J. Baxter and S. Mitragotri, Jet-induced skin puncture and its impact on needle-free jet injections: Experimental studies and a predictive model, J. Controlled Release 106 (2005) 361-373.
[39] B.D. Hemond, A.J. Taberner, N.C. Hogan, B. Crane, and I.W. Hunter, Development and performance of a controllable autoloading needle-free jet injector. J. Med. Dev. 5 (2011) 015001-1-015001-7.
[40] R.M.J. Williams, N.C. Hogan, P.M.F. Nielsen, I.W. Hunter, and A.J. Taberner, A computational model of a controllable needle-free jet injector. 34th IEEE EMBS Annual International Conference (2012) 2052-2055.
[41] R.M.J. Williams, B.P. Ruddy, N.C. Hogan, I.W. Hunter, P.M.F. Nielsen, and A.J. Taberner, Analysis of moving-coil actuator jet injectors for viscous fluids. IEEE Transactions on Biomedical Engineering 63 (2016) 1099-1106.
[42] W.C. Hanly, B.T. Bennett, and J.E. Artwohl, Adjuvants and their use. Part II. BRL Bulletin 9(9) (1994) 1-4.
[43] E.B. Lindblad, Aluminium compounds for use in vaccines. Immuno. Cell Bio. 82 (2004) 497-505.
[43] L.T.S. Jones, L.J. Peek, J. Power, A. Markham, B. Yazzie, and C.R. Middaugh, Effects of adsorption to aluminum salt adjuvants on the structure and stability of model protein antigens, J. Bio. Chem. 280(14) (2005) 13406-13414.
[44] R.K. Gupta, Aluminum compounds as vaccine adjuvants, Adv. Drug Delivery Rev. 32 (1998) 155-172.
[46] J.M. Cregg, J.F. Tschopp, C. Stillman, R. Siegel, M. Akong, W.S. Craig, R.G. Buckholz, K.R. Madden, P.A. Kellaris, G.R. Davis, B.L. Smiley, J.Cruze, R. Torregrossa, G. Velicelebi, and F.P. Thill, High-level expression and efficient assembly of hepatitis B surface antigen in the methylotrophic yeast, Pichia Pastoris, Nature Biotechnology 5 (1987) 479-485.
[47] P. Tollais, C. Pourcel, and A. Dejean, The hepatitis B virus, Nature 317 (1985) 489-495.

[48] M. Omata, C.T. Liew, M. Ashcavai, and R.L. Peters, Nonimmunologic binding of horseradish peroxidase to hepatitis B surface antigen. A possible source of error in immunohistochemistry, Am. J. Clin. Pathol. 73 (1980) 626-632.
[49] A. Frey, J. Di Canzio, and D. Zurakowski, A statistically defined endpoint titer determination method for immunoassays, J. Immunol.Methods 221 (1998) 35-41.
[50] K. Miura, A.C. Orcutt, O.V. Muratova, L.H. Miller, A. Saul, and C.A. Long, Development and characterization of a standardized ELISA including a reference serum on each plate to detect antibodies induce by experimental malaria vaccines, Vaccine 26(2) (2008) 193-200.
[51] N.P. Demas, A contact force sensor for medical jet injection (MS thesis), Dept. Mechanical Engineering, MIT 2015.